Study of the decay $\phi \to \eta\pi^0\gamma$ with the KLOE detector

KLOE Collaboration

A. Aloisio[e], F. Ambrosino[e], A. Antonelli[b], M. Antonelli[b], C. Bacci[j], G. Bencivenni[b], S. Bertolucci[b], C. Bini[h], C. Bloise[b], V. Bocci[h], F. Bossi[b], P. Branchini[j], S.A. Bulychjov[o], G. Cabibbo[h], R. Caloi[h], P. Campana[b], G. Capon[b], G. Carboni[i], M. Casarsa[l], V. Casavola[d], G. Cataldi[d], F. Ceradini[j], F. Cervelli[f], F. Cevenini[e], G. Chiefari[e], P. Ciambrone[b], S. Conetti[m], E. De Lucia[h], G. De Robertis[a], P. De Simone[b], G. De Zorzi[h], S. Dell'Agnello[b], A. Denig[b], A. Di Domenico[h], C. Di Donato[e], S. Di Falco[c], A. Doria[e], M. Dreucci[b], O. Erriquez[a], A. Farilla[j], G. Felici[b], A. Ferrari[j], M.L. Ferrer[b], G. Finocchiaro[b], C. Forti[b], A. Franceschi[b], P. Franzini[h], C. Gatti[f], P. Gauzzi[h], S. Giovannella[b], E. Gorini[d], F. Grancagnolo[d], E. Graziani[j], S.W. Han[b,n], X. Huang[b,n], M. Incagli[f], L. Ingrosso[b], W. Kluge[c], C. Kuo[c], V. Kulikov[o], F. Lacava[h], G. Lanfranchi[b], J. Lee-Franzini[b,k], D. Leone[h], F. Lu[b,n], C. Luisi[h], M. Martemianov[c], M. Matsyuk[b,o], W. Mei[b], L. Merola[e], R. Messi[i], S. Miscetti[b], M. Moulson[b], S. Müller[c], F. Murtas[b], M. Napolitano[e], A. Nedosekin[b,o], F. Nguyen[j], M. Palutan[b], L. Paoluzi[i], E. Pasqualucci[h], L. Passalacqua[b], A. Passeri[j], V. Patera[b,g], E. Petrolo[h], G. Pirozzi[e], L. Pontecorvo[h], M. Primavera[d], F. Ruggieri[a], P. Santangelo[b], E. Santovetti[i], G. Saracino[e], R.D. Schamberger[k], B. Sciascia[b], A. Sciubba[b,g], F. Scuri[l], I. Sfiligoi[b], T. Spadaro[b], E. Spiriti[j], G.L. Tong[b,n], L. Tortora[j], E. Valente[h], P. Valente[b], B. Valeriani[c], G. Venanzoni[f], S. Veneziano[h], A. Ventura[d], Y. Xu[b,n], Y. Yu[b,n]

[a] *Dipartimento di Fisica dell'Università e Sezione INFN, Bari, Italy*
[b] *Laboratori Nazionali di Frascati dell'INFN, Frascati, Italy*
[c] *Institut für Experimentelle Kernphysik, Universität Karlsruhe, Germany*
[d] *Dipartimento di Fisica dell'Università e Sezione INFN, Lecce, Italy*
[e] *Dipartimento di Scienze Fisiche dell'Università "Federico II" e Sezione INFN, Napoli, Italy*
[f] *Dipartimento di Fisica dell'Università e Sezione INFN, Pisa, Italy*
[g] *Dipartimento di Energetica dell'Università "La Sapienza", Roma, Italy*
[h] *Dipartimento di Fisica dell'Università "La Sapienza" e Sezione INFN, Roma, Italy*
[i] *Dipartimento di Fisica dell'Università "Tor Vergata" e Sezione INFN, Roma, Italy*
[j] *Dipartimento di Fisica dell'Università "Roma Tre" e Sezione INFN, Roma, Italy*
[k] *Physics Department, State University of New York at Stony Brook, USA*
[l] *Dipartimento di Fisica dell'Università e Sezione INFN, Trieste, Italy*
[m] *Physics Department, University of Virginia, USA*
[n] *Institute of High Energy Physics, CAS, Beijing, PR China*

[o] *Institute for Theoretical and Experimental Physics, Moscow, Russia*

Abstract

In a sample of 5.3×10^7, ϕ-decays observed with the KLOE detector at the Frascati ϕ-factory DAΦNE we find 605 $\eta\pi^0\gamma$ events with $\eta \to \gamma\gamma$ and 197 $\eta\pi^0\gamma$ events with $\eta \to \pi^+\pi^-\pi^0$. The decay $\eta\pi^0\gamma$ is dominated by the process $\phi \to a_0\gamma$. From a fit to the $\eta\pi^0$ mass spectrum we find BR$(\phi \to a_0(980)\gamma) = (7.4 \pm 0.7) \times 10^{-5}$. © 2002 Elsevier Science B.V. All rights reserved.

PACS: 13.65.+i; 14.40.-n

Keywords: e^+e^- collisions; ϕ radiative decays; Scalar mesons

There is no clear understanding of the $a_0(980)$ and $f_0(980)$ mesons in the quark model. It has been argued that these mesons might not in fact be $q\bar{q}$ states but rather 4-quark states ($q\bar{q}q\bar{q}$) [1] or $K\overline{K}$ molecules [2]. The amplitude for the E1 transition $\phi \to a_0\gamma$ to a state a_0 with $J^P(a_0) = 0^+$ is proportional to $k \times f(m^2)$, with k the momentum and m the mass of the a_0. The differential decay width $d\Gamma/dm$ for $\phi \to a_0\gamma$ has the form $k^2 \times F(m^2)$, where F is a Lorentzian for the a_0 times a damping factor depending on the ϕ and a_0 wave functions. The shape of the a_0 signal in ϕ decay is therefore grossly distorted, acquiring a large tail at low m.

According to different interpretations the $\phi \to a_0\gamma$ branching ratio can range from 10^{-5} for $q\bar{q}$ and $K\overline{K}$ to 10^{-4} for $q\bar{q}q\bar{q}$ [3]. The ratio BR$(\phi \to f_0\gamma)$/BR$(\phi \to a_0\gamma)$ also depends on the structure of the scalars [4]. Chiral perturbation theory also attempts to estimate the amplitude and the distortion of the a_0 line shape observed in ϕ meson decays [5]. Production of the a_0 meson, followed by $a_0 \to \eta\pi^0$ dominates the final state $\eta\pi^0\gamma$ in ϕ-decays. A small contribution is due to $\phi \to \rho^0\pi^0$, $\rho^0 \to \eta\gamma$. We present in the following a study of the decay $\phi \to \eta\pi^0\gamma$ performed with the KLOE detector [6] at the Frascati ϕ-factory [7] DAΦNE. DAΦNE delivered about 16 pb^{-1} during the year 2000, operating at a total energy of 1020 MeV. About 5.3×10^7, ϕ mesons were produced and collected by KLOE. We searched for two

types of events. Type 1 events have five photons from $\phi \to \eta\pi^0\gamma$ with $\eta \to \gamma\gamma$. Type 2 events have five photons plus two charged tracks corresponding to the same initial decay but with $\eta \to \pi^+\pi^-\pi^0$. Observation of type 1 events has been reported by SND [8] and CMD-2 [9] experiments at Novosibirsk. In this work we report the first observation of type 2 events. While the yield for type 2 events is lower, there is no physical background.

The KLOE detector consists of a large cylindrical drift chamber surrounded by a lead-scintillating fiber electromagnetic calorimeter. A superconducting coil provides a 0.52 T field. The drift chamber [10], 4 m in diameter and 3.3 m long, has 12 582 all-stereo tungsten sense wires and 37 746 aluminum field wires. The chamber shell is made of carbon fiber-epoxy composite and the gas used is a 90% helium, 10% isobutane mixture. These features maximize transparency to photons and reduce $K_L \to K_S$ regeneration and multiple scattering. The position resolutions are ≈ 150 μm in the coordinate transverse to the wire direction and ≈ 2 mm in the longitudinal one. The momentum resolution is $\sigma(p_\perp)/p_\perp \approx 0.4\%$. Vertices are reconstructed with a spatial resolution of ≈ 3 mm. The calorimeter [11] is divided into a barrel and two end-caps, for a total of 88 modules, and covers 98% of the solid angle. The modules are read out at both ends by photomultipliers; the read-out granularity is $\sim 4.4 \times 4.4$ cm^2, for a total of 2 440 "cells". The arrival times of particles and the positions in three dimensions of the energy deposits are determined from the signals at the two ends. Cells
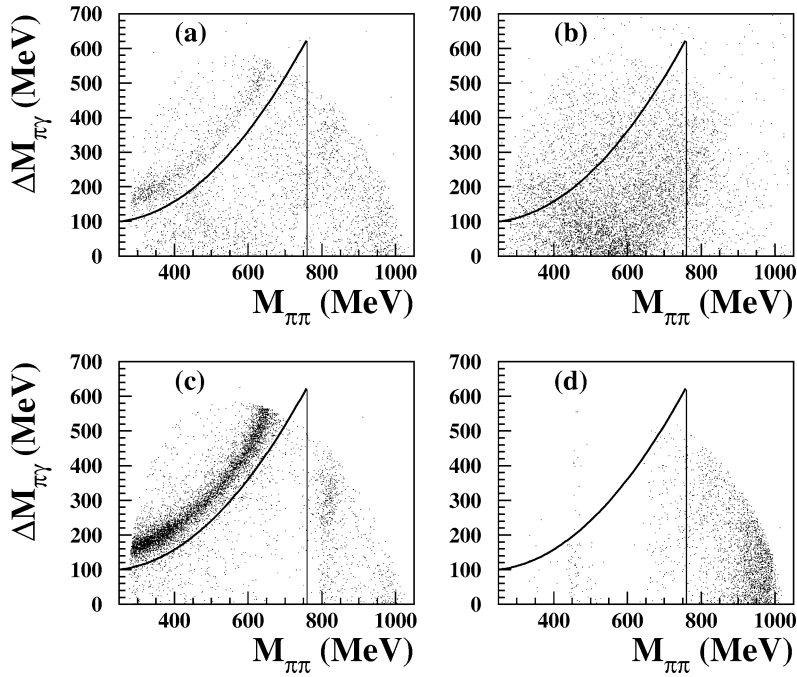
Fig. 1. Invariant mass difference between the two $\pi^0\gamma$ combinations versus the $\pi^0\pi^0$ mass in hypothesis (ii) (see text); (a) data, (b) MC $\phi \to \eta\pi^0\gamma$, (c) MC $e^+e^- \to \omega\pi^0 \to \pi^0\pi^0\gamma$, (d) MC $\phi \to \pi^0\pi^0\gamma$. The solid lines delimit the selected region.

determined from the signals at the two ends. Cells close in time and space are grouped into a calorimeter cluster. The cluster energy E_{CL} is the sum of the cell energies. The cluster time t_{CL} and position $\vec{r}_{CL}$ are energy weighted averages. Time and energy resolutions are $\sigma_E/E = 5.7\%/\sqrt{E \text{ (GeV)}}$ and $\sigma_t = (57 \text{ ps})/\sqrt{E \text{ (GeV)}} \oplus (50 \text{ ps})$, respectively; space resolution is ≈ 1 cm in all the three coordinates. The detector trigger [12] uses calorimeter and chamber information.

We first consider the case of $\phi \to \eta\pi^0\gamma$ decays in which $\eta \to \gamma\gamma$. These events are characterized by five prompt photons. A photon is detected as a calorimeter cluster with $E_{CL} > 3$ MeV, with no track pointing to it, and satisfying $|t_{CL} - |\vec{r}_{CL}|/c| < 5\sigma_t(E_{CL})$. Photons with $|\cos\theta| > 0.93$ are rejected to avoid machine background. Exactly five prompt photons are required. The main background processes are:

(1) $\phi \to \pi^0\pi^0\gamma$ dominated by $\phi \to f_0\gamma$;
(2) $e^+e^- \to \omega\pi^0$ with $\omega \to \pi^0\gamma$;
(3) $\phi \to \eta\gamma$ with $\eta \to \gamma\gamma$;
(4) $\phi \to \eta\gamma$ with $\eta \to \pi^0\pi^0\pi^0$.

Process (3) can mimic five photon events due to energy cluster splitting or accidental background while in process (4) photons can escape detection. Background from $\phi \to K_S K_L$ with $K_S \to \pi^0\pi^0$ and K_L interacting in the calorimeter is negligible after requiring the sum of the energy of the five prompt photons to be greater than 700 MeV. About 1.5×10^4 events survive cuts. A first kinematic fit, in which 4-momentum conservation and $t - |\vec{r}|/c = 0$ for each prompt photon are required, is performed. Background from processes (3) and (4) is reduced by requiring $\chi^2/\text{ndf} < 3$. Events with a $\gamma\gamma$ pair having an invariant mass close to the η mass within 30 MeV are retained. Then events with one of the three remaining photons having energy greater than 340 MeV are rejected to reduce background (3); 2.5×10^3 events remain after cuts.

The best photon pairing is found by matching the invariant masses of the $\gamma\gamma$ pairs to the intermediate particles masses, either (i) η and π^0 or (ii) $2\pi^0$. A second kinematic fit is then performed, with constraints on the masses of the intermediate particles, in both hypotheses. For hypothesis (i) we retain events with
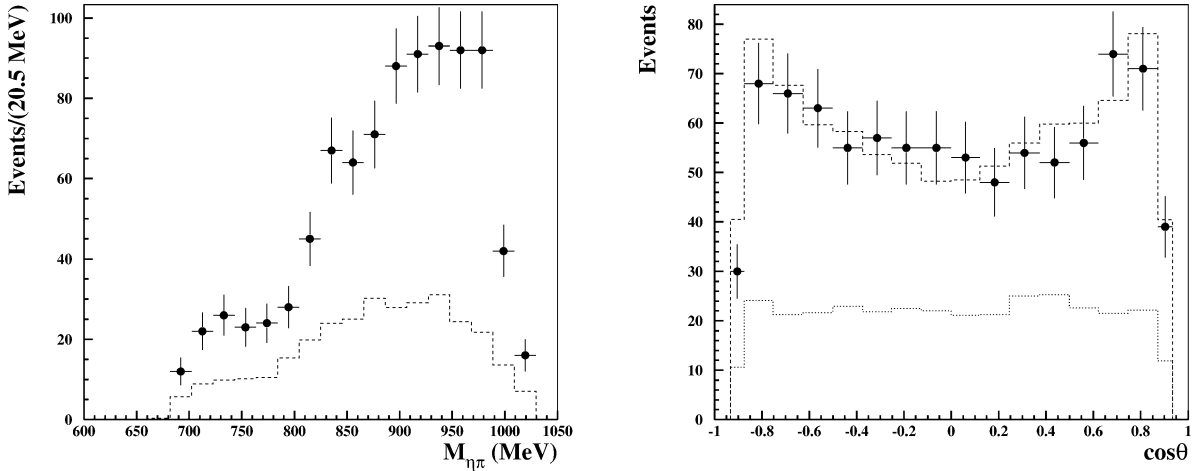
Fig. 2. $\eta \to \gamma\gamma$ sample. Left: $\eta\pi^0$ invariant mass spectrum (points), residual background contribution (dashed histogram); right: $\cos\theta_\gamma$ distribution of the unassociated photon, comparison between data (points) and MC signal (dashed histogram) and MC background (dotted histogram).

$\chi^2/\text{ndf} < 3$. The sample is still dominated by $\pi^0\pi^0\gamma$ events from processes (1) and (2). These two contributions can be discriminated from the signal by exploiting the result of the fit with hypothesis (ii). For each of the two $\pi^0\gamma$ combinations, an invariant mass $M_{\pi\gamma}$ is obtained; in Fig. 1 the absolute value of their difference $\Delta M_{\pi\gamma}$ is plotted versus the $\pi^0\pi^0$ invariant mass $M_{\pi\pi}$, both for data and Montecarlo (MC) events. The $\omega\pi^0$ contribution is represented by the curved band, while $\phi \to \pi^0\pi^0\gamma$ events are mainly located at high values of $M_{\pi\pi}$. In order to select a clean $\phi \to \eta\pi^0\gamma$ sample, the region below the solid curve of Fig. 1 and with $M_{\pi\pi} < 760$ MeV is retained. The final sample consists of 916 events. The spectrum of the $\eta\pi^0$ invariant mass $M_{\eta\pi}$ is shown in Fig. 2 together with the expected distribution for the background. In Fig. 2 the distribution of $\cos\theta_\gamma$ of the unassociated photon is also shown, exhibiting the expected $1 + \cos^2\theta_\gamma$ behaviour. The efficiency for the identification of signal events is evaluated by applying the whole analysis chain to a sample of simulated $\phi \to \eta\pi^0\gamma$ events generated with a uniform $M_{\eta\pi}$ distribution. The selection efficiency as a function of $M_{\eta\pi}$ is shown in Fig. 3. The average over the whole mass spectrum is 32.4%. The background rejection factors and the expected number of events, as obtained by MC simulation, are given in Table 1. The total number is 309 ± 20 background events.
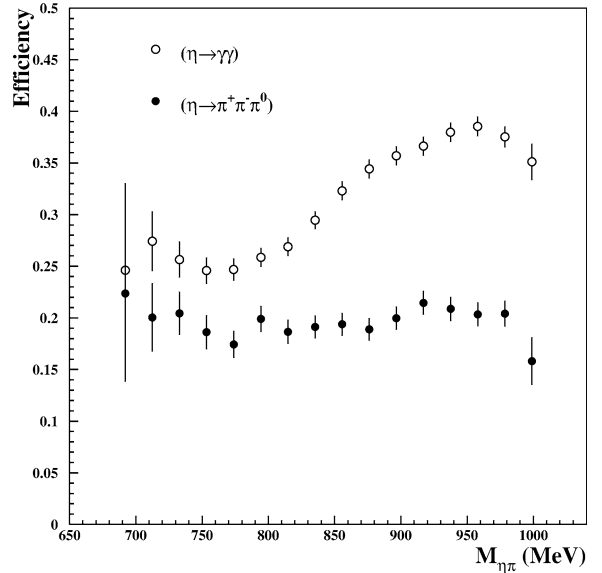

Fig. 3. Selection efficiency as a function of $M_{\eta\pi}$ for type 1 and type 2 final states.

We next consider the case of $\eta\pi^0\gamma$ in which $\eta \to \pi^+\pi^-\pi^0$. This decay chain gives a final state with 2 charged pions and 5 prompt photons. This signature is unique among the possible final states so that the main background sources come from final states with similar topologies and much larger branching ratios. The most significant backgrounds are:
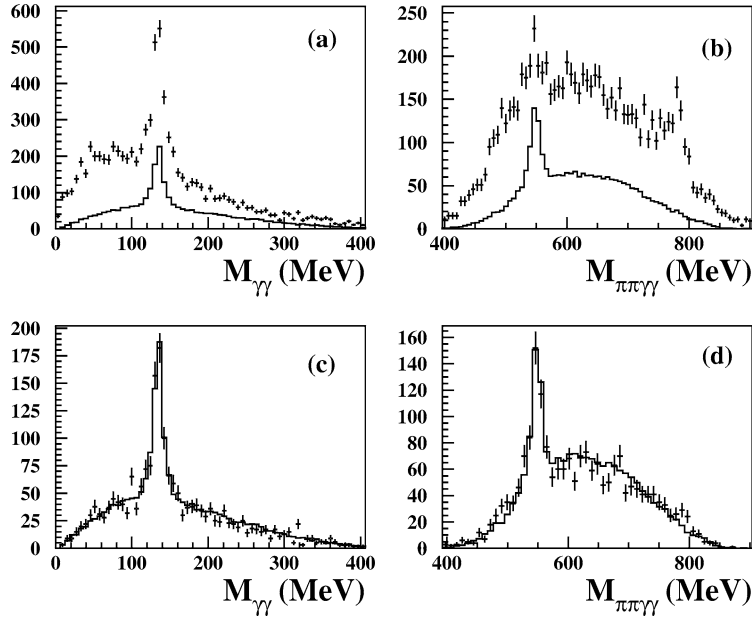
Fig. 4. Distributions of the invariant mass of all $\gamma\gamma$ and $\pi^+\pi^-\gamma\gamma$ combinations for the events surviving fit1 ((a) and (b)) and fit2 ((c) and (d)). The distributions are compared with the MC ones (histograms) for the signal only.

Table 1
Rejection factors for the background processes contributing to the five photon final state. The errors on the number of expected events include MC statistics and systematics from cross section uncertainties

Process	Rejection factor	Expected events
$e^+e^- \to \omega\pi^0 \to \pi^0\pi^0\gamma$	140	54 ± 6
$\phi \to \pi^0\pi^0\gamma$	40	152 ± 16
$\phi \to \eta\gamma \to \gamma\gamma\gamma$	6×10^4	5 ± 2
$\phi \to \eta\gamma \to \pi^0\pi^0\pi^0\gamma$	2.5×10^3	98 ± 10

- $\phi \to \eta\gamma$ with $\eta \to \pi^+\pi^-\pi^0$ (2 tracks and 3 photons);
- $e^+e^- \to \omega\pi^0$ with $\omega \to \pi^+\pi^-\pi^0$ (2 tracks and 4 photons);
- $\phi \to K_S K_L$ with a prompt K_L decay and a combination of $K_S \to \pi^+\pi^-$ and $K_L \to \pi^0\pi^0\pi^0$ or $K_S \to \pi^0\pi^0$ and $K_L \to \pi l\nu$ or $K_L \to \pi^+\pi^-\pi^0$ resulting in 2 tracks and 4 or 6 photons.

The signal events are selected by requiring a vertex close to the interaction region with two tracks of opposite charge, and five prompt photons with $E_\gamma > 10$ MeV and $|\cos\theta| < 0.93$. The surviving events (7.1×10^3) enter a two-step kinematic fit

procedure: a first fit (fit1) with energy/momentum conservation at the vertex, and a second fit (fit2) with π^0 and η mass constraints, where the combination resulting in the higher χ^2 probability is selected. The invariant mass distributions for all $\gamma\gamma$ and $\pi^+\pi^-\gamma\gamma$ combinations are shown in Fig. 4(a) and (b) for the events surviving fit1. A clear η signal already emerges at this stage over a large combinatorial background due to residual $\omega\pi^0$ and $K_S K_L$ events (see the peak close to the ω mass in Fig. 4(b)). After fit2 the residual background is reduced to 4 ± 4 events from $\omega\pi^0$ and less than 8 events from the other possible background modes. Fig. 4(c) and (d) shows the $\gamma\gamma$ and $\pi^+\pi^-\gamma\gamma$ invariant mass distributions at this stage compared with the MC distributions for the signal normalized to the same number of events. The comparison shows good agreement. The distribution of $M_{\eta\pi}$ for the 197 events found is shown in Fig. 5(a). The angular distribution of the radiated photon, Fig. 5(b), agrees with $(1 + \cos^2\theta_\gamma)$.

The efficiency (see Fig. 3) as a function of $M_{\eta\pi}$ is found by using MC simulation. Both photon and track efficiencies are corrected using data control samples. ($K_S \to \pi^+\pi^-$ for tracking and $e^+e^-\gamma$ for γ's). The overall efficiency, on average 19%, is dominated by
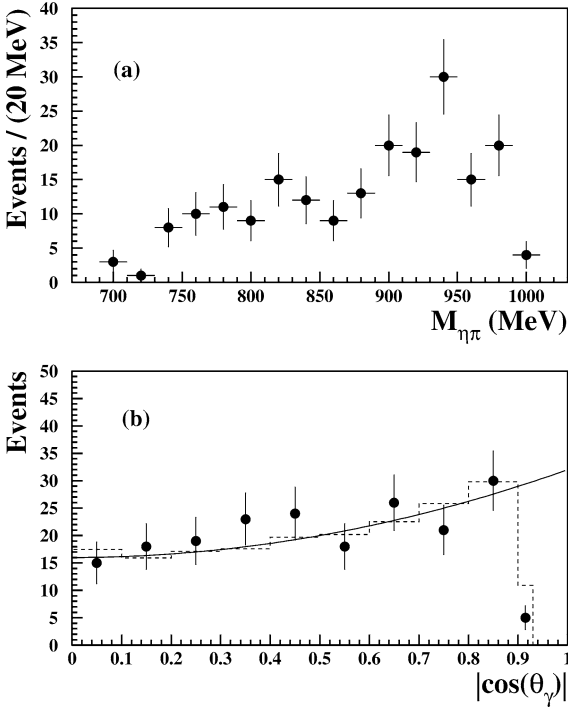
Fig. 5. $\eta \to \pi^+\pi^-\pi^0$ sample. (a) Distribution of the $\eta\pi^0$ invariant mass for the final sample of events; (b) distribution of $|\cos(\theta_\gamma)|$ for the final sample of events. The dashed histogram is the MC, and the curve superimposed corresponds to a $(1 + \cos^2(\theta_\gamma))$ dependence.

the probability for at least one of the seven particles to go out of acceptance. The resolution in $M_{\eta\pi}$ is 4 MeV over the entire mass range. A non-Gaussian tail of about 10% is present, due to incorrect photon pairings.

The $\phi \to \eta\pi^0\gamma$ branching ratio is obtained independently for each sample, normalizing the number of events after background subtraction, $N - B$, to the ϕ cross section σ_ϕ, to the selection efficiency ϵ, and to the integrated luminosity L:

$$\mathrm{BR}(\phi \to \eta\pi^0\gamma) = \frac{N - B}{\epsilon \times \mathrm{BR}(\eta \to i)} \frac{1}{\sigma_\phi L}, \qquad (1)$$

where $i = \gamma\gamma$, $\pi^+\pi^-\pi^0$ and $\mathrm{BR}(\eta \to i)$ is from Ref. [13]. The luminosity is measured using large angle Bhabha scattering events. The σ_ϕ measurement is obtained using the $\phi \to \eta\gamma \to \gamma\gamma\gamma$ decay [14].

We obtain for the sample in which $\eta \to \gamma\gamma$

$$\mathrm{BR}(\phi \to \eta\pi^0\gamma) = (8.51 \pm 0.51_{\mathrm{stat}} \pm 0.57_{\mathrm{syst}}) \times 10^{-5}$$

Table 2
Contributions to the uncertainties in $\mathrm{BR}(\phi \to \eta\pi^0\gamma)$ measurement (10^{-5} units)

	Type 1	Type 2
Statistics	0.43	0.58
Background subtraction	0.28	0.15
Efficiency	0.51	0.30
$\mathrm{BR}(\eta \to x)$	0.05	0.14
Luminosity	0.17	0.16
ϕ cross section	0.17	0.16

and for the sample in which $\eta \to \pi^+\pi^-\pi^0$

$$\mathrm{BR}(\phi \to \eta\pi^0\gamma) = (7.96 \pm 0.60_{\mathrm{stat}} \pm 0.40_{\mathrm{syst}})$$
$$\times 10^{-5}.$$

The two values are in agreement. Our results also agree with those from SND $(8.8 \pm 1.4 \pm 0.9) \times 10^{-5}$ [8] and CMD-2 $(9.0 \pm 2.4 \pm 1.0) \times 10^{-5}$ [9]. Contributions to the uncertainties are listed in Table 2.

We estimate the contribution of $\phi \to a_0\gamma$ from a simultaneous fit of the two $M_{\eta\pi}$ spectra. Two contributions are considered in the fit: (a) $\phi \to \rho^0\pi^0$, $\rho^0 \to \eta\gamma$ and (b) $\phi \to a_0\gamma$, $a_0 \to \eta\pi^0$. The contribution from the continuum process $e^+e^- \to \omega\pi^0$, $\omega \to \eta\gamma$ is negligible due to the low cross section. The $M_{\eta\pi}$ spectrum for (a) is taken from VMD calculations [15,16]. For (b) we use the formulation of Ref. [17] based on ϕ coupling to a charged kaon loop:

$$\frac{\mathrm{d}\Gamma(\phi \to a_0\gamma \to \eta\pi^0\gamma)}{\mathrm{d}M_{\eta\pi}} = \frac{2M_{\eta\pi}^2}{\pi} \frac{\Gamma_{\phi a_0\gamma} \Gamma_{a_0\eta\pi^0}}{|D_{a_0}|^2}, \qquad (2)$$

where $\Gamma_{\phi a_0\gamma}$ is related to the coupling $g_{a_0 K^+ K^-}^2/4\pi$, $\Gamma_{a_0\eta\pi^0}$ to the coupling $g_{a_0\eta\pi^0}^2/4\pi$, and D_{a_0} is the inverse a_0 propagator including finite width corrections. The model assumes point-like couplings.

The efficiency and resolution functions, including distortions from incorrect photon pairings are folded into the theoretical distribution. The experimental spectra after background subtraction (Fig. 6) are simultaneously fitted, setting $M_{a_0} = 984.8$ MeV, from Ref. [13]. The free parameters of the fit are the branching ratio for contribution (a) and the two coupling constants above. We find $\mathrm{BR}(\phi \to \rho^0\pi^0, \rho^0 \to \eta\gamma) = (0.5 \pm 0.5) \times 10^{-5}$, $g_{a_0 K^+ K^-}^2/4\pi = (0.40 \pm 0.04)$ GeV^2, and $g_{a_0\eta\pi}/g_{a_0 K^+ K^-} = 1.35 \pm 0.09$. The contribution from $\phi \to a_0\gamma$ is dominant and that from
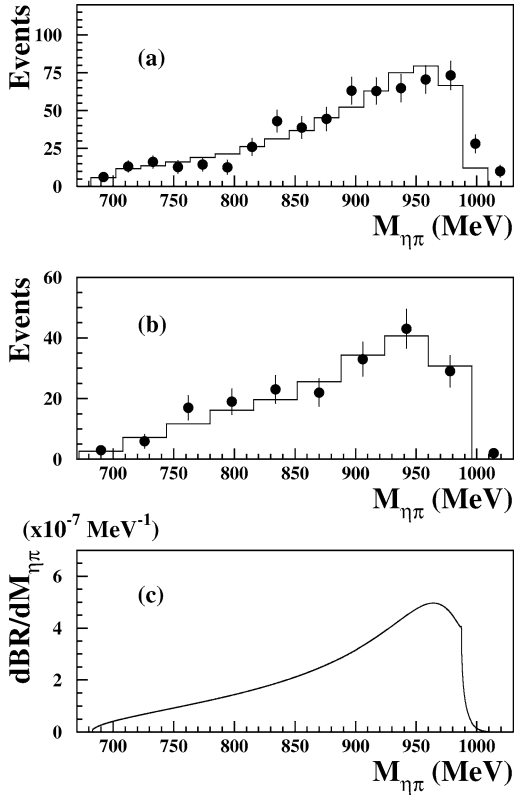
Fig. 6. Result of the combined fit: (a) comparison of data (exp. points) vs. fit (histogram) for (a) type 1 (b) type 2 samples and (c) plot of the theoretical curve for the a_0 contribution with the parameters extracted from the fit.

$\rho^0 \pi^0$ is consistent with zero, in agreement with VMD calculations [16]. By integration we find:

$$\mathrm{BR}\big(\phi \to a_0\gamma, a_0 \to \eta\pi^0\big) = (7.4 \pm 0.7) \times 10^{-5}. \quad (3)$$

The fit is good, with $\chi^2/\mathrm{ndf} = 27.2/25$. Fig. 6 shows the fit and the a_0 contribution. Interference between (a) and (b) has been considered [15] giving no significant effect in the fit results.

The result for $g_{a_0\eta\pi}/g_{a_0 K^+ K^-}$ can be compared with the value 1.05 ± 0.06 given by experiment BNL852 [18] and with the Crystal Barrel results (1.07 or 0.93 depending on the analysis [19]). It can also be compared with expectations based on the standard $q\bar{q}$ model (1.51 according to [17]) and on the $q\bar{q}q\bar{q}$ model (0.93 according to [1]).

Finally, the results are combined with those obtained in the analysis of $\phi \to \pi^0\pi^0\gamma$ [20] done on the same data sample:

- $\mathrm{BR}(\phi \to f_0\gamma \to \pi^0\pi^0\gamma) = (1.49 \pm 0.07) \times 10^{-4}$;
- $g^2_{f_0 K^+ K^-}/4\pi = 2.79 \pm 0.12 \ \mathrm{GeV}^2$.

Multiplying the branching ratio above by a factor of 3 to account for $f_0 \to \pi^+\pi^-$ decays $\mathrm{BR}(\phi \to f_0\gamma)$ is then $(4.47 \pm 0.21) \times 10^{-4}$, and the ratio of the two branching ratios is

$$R_{\mathrm{BR}} = \frac{\mathrm{BR}(\phi \to f_0\gamma)}{\mathrm{BR}(\phi \to a_0\gamma)} = 6.1 \pm 0.6. \quad (4)$$

The ratio of the two couplings to the KK system is

$$R_{g^2} = \frac{g^2_{f_0 KK}}{g^2_{a_0 KK}} = 7.0 \pm 0.7. \quad (5)$$

These ratios are useful for shedding light on the possible sizes and mixing or other structure questions regarding these mesons [4,21].

Acknowledgements

References

[1] R.L. Jaffe, Phys. Rev. D 15 (1977) 267;
M. Alford, R.L. Jaffe, Nucl. Phys. B 578 (2000) 367.

[2] J. Weinstein, N. Isgur, Phys. Rev. Lett. 48 (10) (1982) 659;
F.E. Close, N. Isgur, S. Kumano, Nucl. Phys. B 389 (1993) 513;
N.N. Achasov, V.V. Gubin, V.I. Shevchenko, Phys. Rev. D 56 (1997) 203.

[3] N. Brown, F.E. Close, in: L. Maiani, G. Pancheri, N. Paver (Eds.), Second DAFNE Physics Handbook, Vol. 2, 1995, p. 649;
N.N. Achasov, V.V. Gubin, Phys. Rev. D 56 (1997) 4084.

[4] F.E. Close, A. Kirk, Phys. Lett. B 515 (2001) 13.

[5] E. Marco et al., Phys. Lett. B 470 (1999) 20;
    A. Bramon et al., Phys. Lett. B 494 (2000) 1.

[6] KLOE Collaboration, A. Aloisio et al., KLOE: A General
    Purpose Detector for DAFNE, LNF-92/019 (IR);
    KLOE Collaboration, A. Aloisio et al., The KLOE Detector,
    Technical Proposal, LNF-93/002 (IR).

[7] S. Guiducci, Status of DAΦNE, in: P. Lucas, S. Webber (Eds.),
    Proc. of the 2001 Particle Accelerator Conference, Chicago,
    IL, USA, 2001, pp. 353–355.

[8] M.N. Achasov et al., Phys. Lett. B 479 (2000) 53.

[9] R.R. Akhmetshin et al., Phys. Lett. B 462 (1999) 380.

[10] KLOE Collaboration, M. Adinolfi et al., The KLOE drift
    chamber, submitted to Nucl. Instrum. Methods.

[11] KLOE Collaboration, M. Adinolfi et al., Nucl. Instrum. Meth-
    ods A 482 (1–2) (2002) 364.

[12] KLOE Collaboration, M. Adinolfi et al., The KLOE trigger
    system, submitted to Nucl. Instrum. Methods.

[13] D. Groom et al., Eur. Phys. J. C 15 (2000) 1.

[14] S. Giovannella, S. Miscetti, KLOE Note n. 177, 2002.

[15] N.N. Achasov, V.V. Gubin, Phys. Rev. D 63 (2001) 094007.

[16] A. Bramon, A. Grau, G. Pancheri, Phys. Lett. B 283 (1992)
    416.

[17] N.N. Achasov, V.I. Ivanchenko, Nucl. Phys. B 315 (1989) 465.

[18] S. Teige et al., Phys. Rev. D 59 (2001) 012001.

[19] C. Amsler et al., Phys. Lett. B 333 (1994) 277;
    D.V. Bugg et al., Phys. Rev. D 50 (1994) 4412.

[20] KLOE Collaboration, A. Aloisio et al., hep-ex/0204013, sub-
    mitted to Phys. Lett. B.

[21] N.N. Achasov, A.V. Kiselev, hep-ph/0203042.